ChemComm

COMMUNICATION

View Article Online
View Journal | View Issue

Cite this: *Chem. Commun.*, 2015, **51**, 16123

Received 2nd August 2015,
Accepted 15th September 2015

DOI: 10.1039/c5cc06463e

www.rsc.org/chemcomm

A new Ru,Ru,Pt supramolecular architecture for photocatalytic H_2 production†

Jessica Knoll White*‡ and Karen J. Brewer§

A new polyazine-bridged RuRuPt trimetallic supramolecular architecture emulates the photophysical properties of the previously reported Ru_2RuPt tetrametallic architecture that exhibits photoinduced charge separation. The RuRuPt complexes are more robust H_2O reduction photocatalysts with enhanced stability compared to the Ru_2RuPt tetrametallic analogues.

Solar-to-chemical energy conversion is an important topic in the quest for clean and renewable energy.[1–5] Converting H_2O to H_2 fuel by harvesting solar energy is a complicated multi-electron process that involves bond breaking and formation.[1,6–8] Ru(II)–polyazine complexes, such as the prototypical $[Ru(bpy)_3]^{2+}$ (bpy = 2,2′-bipyridine), are attractive light absorbers (LA) for harnessing solar energy due to their broad UV and visible light absorption and long-lived, strongly reducing/oxidizing excited states.[9–12] Molecular photocatalysts provide a means for analysing and understanding the complicated processes involved in H_2O reduction.[13]

Supramolecular complexes,[14] individual components each possessing their own function assembled into systems that perform a complex task, are an important class of molecular photocatalysts for H_2 production from H_2O. Several supramolecular photocatalysts featuring a Ru–polyazine LA coupled to a reactive metal (RM) such as Co,[15] Rh,[16–21] Pd,[22–24] and Pt,[25–29] are reported. The photocatalytic activity of a series of Ru,Pt bimetallic complexes, $[(bpy)_2Ru\{phenNHCO(Rbpy)\}PtCl_2]^{2+}$ (phen = 1,10-phenanthroline, R = –COOH, –COOEt, or $–CH_3$) depends on the nature of R. The charge separated (CS) excited state is most stabilized in the –COOH complex, providing the greatest activity in aqueous solution with 5 TON in 10 h.[25,27] Dimerization of this architecture through the R-bpy unit doubles the efficiency by enhancing Pt–Pt dimerization for proton coupled electron transfer. A Ru,Pt bimetallic system $[(^tBu_2bpy)_2Ru(tpphz)PtX_2]^{2+}$ ($^tBu_2bpy$ = 4,4′-di-*tert*-butyl-2,2′-bipyridine; tpphz = tetrapyrido-[3,2-*a*:2′,3′-*c*:3″,2″-*h*:2‴,3‴-*j*]phenazine; X = Cl^- or I^-) produces H_2 from H_2O with 7 TON when X = Cl^-, while a 40 fold increase in TON and enhanced stability is achieved when X = I^-.[30] It was recently discovered that the active catalyst of the $Pd^{II}Cl_2$ analogue, $[(^tBu_2bpy)_2Ru(tpphz)PdCl_2]^{2+}$, is colloidal Pd,[31] corroborating results of a previously reported Ru,Pd photocatalyst.[32]

The supramolecular architecture $[\{(TL)_2Ru(dpp)\}_2Ru(BL)PtCl_2]^{6+}$ (Ru_2RuPt; TL = phen or Ph_2phen = 4,7-diphenyl-1,10-phenanthroline; BL = dpp = 2,3-bis(2-pyridyl)pyrazine or dpq = 2,3-bis(2-pyridyl)-quinoxaline) is active in photocatalytic H_2 production from H_2O by virtue of photoinduced charge separation in which the HOMO is localized on the terminal Ru and the LUMO is localized on BL coordinated to the Pt RM.[33,34] The catalytic efficiency of this architecture is strongly influenced by the nature of BL; the complexes with BL = dpq display greatly enhanced catalysis compared to their BL = dpp counterparts owing to the stabilized LUMO and enhanced driving force for intramolecular electron transfer toward the reactive Pt centre. Spectroscopic analysis of these complexes is difficult due to the presence of multiple overlapping, strongly absorbing intraligand (IL) $\pi \rightarrow \pi^*$ and metal-to-ligand charge transfer (MLCT) transitions in the UV and visible regions, respectively.

Reported herein is the new trimetallic supramolecular architecture $[(Ph_2phen)_2Ru(dpp)Ru(bpy)(BL)PtCl_2]^{4+}$ (labelled RuRuPt; BL = dpp or dpq) designed to provide analogous redox, spectroscopic, photophysical, and photocatalytic properties compared to the Ru_2RuPt tetrametallic complexes. Reducing the number of $(Ph_2phen)_2Ru^{II}(dpp)$ LA units from two to one simplifies the molecular architecture and provides more active photocatalysts for H_2O reduction compared to the Ru_2RuPt analogues. Fig. 1 depicts the structures of the new RuRuPt trimetallic complexes, $[(Ph_2phen)_2Ru(dpp)Ru(bpy)(dpp)PtCl_2]^{4+}$ (**RuRudppPt**) and $[(Ph_2phen)_2Ru(dpp)Ru(bpy)(dpq)PtCl_2]^{4+}$ (**RuRudpqPt**), and the previously reported Ru_2RuPt tetrametallic complexes (**Ru_2RudppPt** and **Ru_2RudpqPt**). The synthesis, redox and

Department of Chemistry, Virginia Tech, Blacksburg, VA, 24061, USA.
E-mail: knoll.56@osu.edu

† Electronic supplementary information (ESI) available: Experimental details, electrochemical, spectroscopic, and photocatalytic data, three dimensional models. See DOI: 10.1039/c5cc06463e

‡ Current address: Department of Chemistry and Biochemistry, The Ohio State University, Columbus, OH, 43210, USA.

§ Karen J. Brewer is deceased (October 24, 2014).

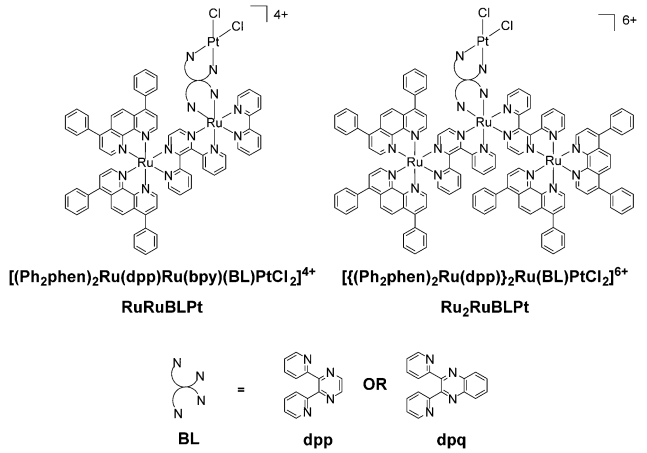

Fig. 1 Structural representations of the RuRuPt and Ru_2RuPt complexes.

spectroscopic properties, and photocatalytic activity towards H_2O reduction of this new architecture are discussed below.

The RuRuPt complexes were assembled using a six step building block process. Synthetic details are provided in ESI.† The synthetic approach to these structurally complicated supramolecules required initial assembly of the bimetallic complex $[(Ph_2phen)_2Ru(dpp)RuCl_2(bpy)](PF_6)_2$ by coupling $[(Ph_2phen)_2Ru(dpp)](PF_6)_2$[35] and $[(bpy)RuCl_2(DMSO)_2]$[36] monometallic precursors. This complex was reacted with either dpp or dpq to provide an open coordination site to extend the molecular architecture, thereby generating bimetallics of the design $[(Ph_2phen)_2Ru(dpp)Ru(bpy)(BL)](PF_6)_4$. The RuRuPt trimetallics, $[(Ph_2phen)_2Ru(dpp)Ru(bpy)(BL)PtCl_2](PF_6)_4$ (**RuRudppPt** and **RuRudpqPt**), were prepared upon reacting the BL-containing bimetallic with *cis*-$[PtCl_2(DMSO)_2]$. ESI-MS data is consistent with the desired product for each complex.

Electrochemical analysis of the RuRuPt complexes and their bimetallic precursors indicates orbital energetics that are similar to the analogous Ru_2RuPt tetrametallic complexes and their trimetallic precursors. Square wave voltammograms are provided in Fig. S1 and the data and assignments are given in Table S1 (ESI†). Fig. 2a highlights the similarities between the cyclic voltammograms of **RuRudpqPt** and **Ru_2RudpqPt**. The new RuRuPt complexes possess the same spatially separated HOMO and LUMO that was reported in the Ru_2RuPt complexes and is necessary for photoinduced charge separation.[33,34,37] The first oxidation process at 1.54–1.57 V *vs.* Ag/AgCl is assigned the terminal $Ru^{II/III}$ oxidation in all four Pt-containing complexes. This couple for **Ru_2RudppPt** and **Ru_2RudpqPt** has approximately twice the peak current of **RuRudppPt** and **RuRudpqPt**, consistent with the number of terminal Ru centres (two and one, respectively). The first reduction is assigned as $BL^{0/-}$; this reduction occurs at −0.39 V and −0.08 V for **RuRudppPt** and **RuRudpqPt**, respectively, and this trend is consistent with dpq's stabilized π* orbitals compared to those of dpp. The $BL^{0/-}$ potentials are quite similar to those of the corresponding tetrametallic complexes (−0.33 V and −0.02 V for **Ru_2RudppPt** and **Ru_2RudpqPt**, respectively). This supports the validity of the RuRuPt complexes as analogues for the Ru_2RuPt complexes.

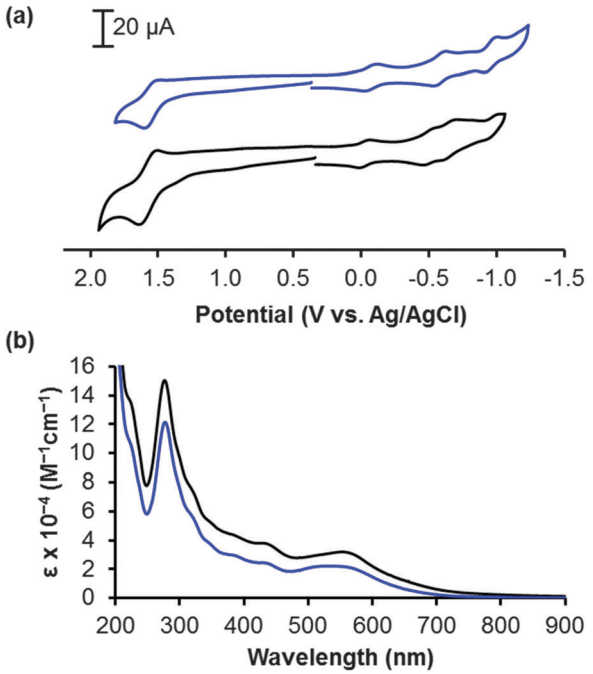

Fig. 2 Cyclic voltammograms measured in CH_3CN with 0.1 M Bu_4NPF_6 (a) and electronic absorption spectra in CH_3CN (b) of **Ru_2RudpqPt** (black) and **RuRudpqPt** (blue).

The electronic absorption spectrum for each of the RuRuPt complexes is similar to the Ru_2RuPt analogue while exhibiting a decrease in the molar absorptivity throughout the UV and visible regions due to the absence of a strongly absorbing $(Ph_2phen)_2Ru^{II}(dpp)$ unit. This is shown in Fig. 2b and Fig. S2 and Table S2 (ESI†). Similar to related Ru(II)–polyazine complexes, the UV and visible regions are dominated by IL and MLCT transitions, respectively, with transitions involving dpp or dpq red-shifted compared to Ph_2phen transitions. The broad, lowest energy absorption band for **RuRudpqPt** is centred at 543 nm (ε = 22 000 M^{-1} cm^{-1}) with contributions from Ru → dpp and Ru → dpq ^{1}MLCT transitions. The lowest energy band for **Ru_2RudpqPt** is centred at 550 nm with ε = 31 000 M^{-1} cm^{-1} due to additional central Ru → dpp and terminal Ru → dpp ^{1}MLCT transitions. Similar trends are observed in comparing **RuRudppPt** with **Ru_2RudppPt** (Table S2, ESI†). The RuRuPt architecture maintains the broad light absorption that covers the entire visible region which is desirable in solar energy conversion, while decreasing the number of possible transitions to allow for further studies such as transient absorption spectroscopy.

The emissive nature of the RuRuPt complexes provides a convenient probe into the excited state dynamics that are similar to those observed for the Ru_2RuPt complexes. A simplified state diagram for **RuRudpqPt** is pictured in Fig. S3 and emission spectroscopy data is presented in Table S3 and Fig. S4 and S5 (ESI†). Emission is observed from the terminal Ru → dpp ^{3}MLCT excited state in each case. The two $[(Ph_2phen)_2Ru(dpp)Ru(bpy)(BL)](PF_6)_4$ bimetallic complexes emit at 762 nm with τ = 120 ns and Φ^{em} = 1.5 × 10^{-3}. These homobimetallics serve as photophysical models to study charge separation in the

Pt-containing complexes. Coordination of *cis*-$PtCl_2$ results in quenched emission ($\Phi^{em} = 1.1 \times 10^{-3}$ and 5.2×10^{-4} for BL = dpp and dpq, respectively) and shortened excited state lifetimes (τ = 90 and 100 ns when BL = dpp and dpq, respectively) as the Pt unit stabilizes the BL(π^*) orbitals and enables intramolecular electron transfer to populate a low-lying, non-emissive charge separated (^{3}CS) state. As observed in the Ru_2RuPt complexes, the degree of emission quenching and charge separation is strongly dependent on the nature of BL.[34,37] The emissive ^{3}MLCT state is populated with 98% and 43% efficiency for **RuRudppPt** and **RuRudpqPt** with λ^{exc} = 540 nm (equations in ESI†). These efficiencies are close to the analogous Ru_2RuPt complexes (99% and 51% for **Ru_2RudppPt** and **Ru_2RudpqPt**, respectively).[34] Less efficient emissive state population results from more efficient population of the ^{3}CS state. The degree by which Φ^{em} and τ of the ^{3}MLCT state are quenched varies substantially due to population of the ^{3}CS from both the emissive ^{3}MLCT state and a higher-energy ^{3}MLCT state, as discussed previously.[34,37] The agreement in photophysical properties of the Ru_2RuPt and RuRuPt complexes further demonstrates the suitability of the new architecture as analogues to the tetrametallic complexes.

The RuRuPt complexes exhibit remarkably enhanced photocatalytic activity and stability towards H_2 production from H_2O compared to their Ru_2RuPt analogues. Table 1 features the amount of H_2 produced and turnover number (TON = moles of H_2 produced/moles of catalyst) for **RuRudppPt** and **RuRudpqPt** as well as for the previously reported **Ru_2RudppPt** and **Ru_2RudpqPt** following 470 nm irradiation (flux = 2.3×10^{19} photons per min) for 20 hours in RT CH_3CN with 50 μM metal complex, 0.62 M H_2O, 1.5 M DMA sacrificial electron donor, and 110 μM [$DMAH^+$][$SO_3CF_3^-$]. The volume of the solution and the headspace are 4.5 mL and 15.3 mL, respectively. The reported values are the average of three experiments. To highlight the greater activity of the new architecture, a plot of H_2 production *vs.* time for **RuRudpqPt** and **Ru_2RudpqPt** is provided in Fig. 3, and the plot for the dpp analogues are provided in Fig. S6 (ESI†). **RuRudpqPt** is the most active catalyst in this series, producing 52 ± 4 μmol of H_2 in 20 hours and undergoing 230 ± 20 TON (quantum yield of H_2 production, $\Phi = 1.1 \times 10^{-3}$). The enhancement in photocatalytic activity within the trimetallic series of **RuRudpqPt** and **RuRudppPt** (29 ± 2 μmol of H_2, 130 ± 9 TON, $\Phi = 6.2 \times 10^{-4}$) is related to the enhanced ^{3}CS state population in the BL = dpq complex and agrees with the trend observed in the analogous Ru_2RuPt complexes.[34] For each BL, the H_2 production of the RuRuPt complex is greater than the Ru_2RuPt analogue (shown in Fig. 3 for the BL = dpq analogues) despite the smaller molecule's less efficient absorption at 470 nm. The RuRuPt architecture is expected to provide less demanding steric bulk near the *cis*-$PtCl_2$ site, whereas the presence of two bulky $(Ph_2phen)_2Ru^{II}$(dpp) units in the Ru_2RuPt architecture may hinder interactions between the substrate and the catalytic site. Three dimensional models highlighting the difference in sterics for different geometric isomers of the **Ru_2RudpqPt** and **RuRudpqPt** architectures are provided in Fig. S7 (ESI†). The RuRuPt and Ru_2RuPt complexes are expected to exist in up to 16 and 32 isomers, respectively, as a result of Λ and Δ optical isomers as well as the AB chelating nature of the bridging ligands. The distribution of isomers in each sample is unknown; however, steric effects on reactivity, charge separation distance, and orbital overlap are expected to result from structural variations among isomers.

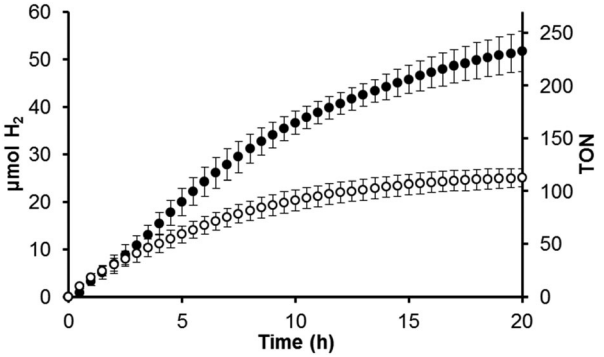

Fig. 3 Photocatalytic H_2 production with **RuRudpqPt** (black circles) and **Ru_2RudpqPt** (white circles) with 50 μM catalyst in spectral grade CH_3CN, 0.62 M H_2O, 1.5 M DMA, and 110 μM [$DMAH^+$][$SO_3CF_3^-$]. Solutions were irradiated with λ = 470 ± 10 nm.

Table 1 Photocatalytic H_2 production data for RuRuPt and Ru_2RuPt supramolecular complexes[a]

Complex	μmol H_2	TON[b]	$\Phi^c \times 10^4$
Ru_2RudppPt	7.1 ± 3.2	32 ± 14	1.6 ± 0.7
Ru_2RudpqPt	25 ± 1	110 ± 6	5.5 ± 0.3
RuRudppPt	29 ± 2	130 ± 9	6.2 ± 0.4
RuRudpqPt	52 ± 4	230 ± 20	11 ± 1

[a] 50 μM catalyst in spectral grade CH_3CN, 0.62 M H_2O, 1.5 M DMA, 110 μM [$DMAH^+$][$SO_3CF_3^-$], λ_{irr} = 470 ± 10 nm (flux = 2.3×10^{19} photons per min). Values represent H_2 production after 20 h photolysis. [b] TON = moles of H_2 produced/moles of catalyst. [c] Quantum yield of H_2 production.

The new RuRuPt trimetallic supramolecular architecture features a Ru(II)–polyazine LA and a *cis*-$PtCl_2$ RM site with a spatially separated HOMO and LUMO that imparts unusual photophysical properties. This architecture provides redox and photophysical properties analogous to the previously reported Ru_2RuPt architecture, demonstrating the ability to design supramolecular complexes with desired properties through knowledge of previously studied systems. The architecture features a terminal Ru-based HOMO and a remote BL-based LUMO which enables photoinduced charge separation. The nature of BL dictates the energy of the LUMO and largely impacts the population of the ^{3}CS state in competition with population of the emissive ^{3}MLCT state, with BL = dpq affording a complex with a more efficiently populated ^{3}CS state compared to the BL = dpp analogue. The enhanced charge separation in **RuRudpqPt** is important in providing an active and stable catalyst for H_2 production from H_2O (52 μmol of H_2 and 230 TON in 20 h) while **RuRudppPt** is less active (29 μmol of H_2 and 130 TON in 20 h). Both of these complexes are superior to their Ru_2RuPt analogues, possibly due to steric factors provided by the bulky $(Ph_2phen)_2Ru^{II}$(dpp) units or a varied distribution of geometric isomers. Future studies include further probing the unusual excited state dynamics using transient absorption spectroscopy enabled by the less complicated spectroscopy by virtue of the absence of a strongly absorbing LA unit.

Acknowledgement is made to the Chemical Sciences, Geosciences and Biosciences Division, Office of Basic Energy Sciences, Office of Sciences, U.S. Department of Energy (DE FG02-05ER15751) for their generous support of the development of new LAs used in this research.

References

1 A. J. Bard and M. A. Fox, *Acc. Chem. Res.*, 1995, **28**, 141–145.
2 D. Gust and T. A. Moore, *Science*, 1989, **244**, 35–41.
3 D. Gust, T. A. Moore and A. L. Moore, *Acc. Chem. Res.*, 2009, **42**, 1890–1898.
4 N. S. Lewis and D. G. Nocera, *Proc. Natl. Acad. Sci. U. S. A.*, 2006, **103**, 15729–15735.
5 N. D. McDaniel and S. Bernhard, *Dalton Trans.*, 2010, **39**, 10021–10030.
6 N. Armaroli and V. Balzani, *ChemSusChem*, 2011, **4**, 21–36.
7 M. Grätzel, *Acc. Chem. Res.*, 1981, **14**, 376–384.
8 W. Lubitz and W. Tumas, *Chem. Rev.*, 2007, **107**, 3900–3903.
9 B. Durham, J. V. Caspar, J. K. Nagle and T. J. Meyer, *J. Am. Chem. Soc.*, 1982, **104**, 4803–4810.
10 K. Kalyanasundaram, *Coord. Chem. Rev.*, 1982, **46**, 159–244.
11 T. J. Meyer, *Pure Appl. Chem.*, 1986, **58**, 1193–1206.
12 R. J. Watts, *J. Chem. Educ.*, 1983, **60**, 834–842.
13 A. J. Esswein and D. G. Nocera, *Chem. Rev.*, 2007, **107**, 4022–4047.
14 V. Balzani, L. Moggi and F. Scandola, in *Supramolecular Photochemistry*, ed. V. Balzani, NATO ASI Series 214, Reidel, Dordrecht, The Netherlands, 1987, pp. 1–28.
15 A. Fihri, V. Artero, M. Razavet, C. Baffert, W. Leibl and M. Fontecave, *Angew. Chem., Int. Ed.*, 2008, **47**, 564–567.
16 M. Elvington, J. Brown, S. M. Arachchige and K. J. Brewer, *J. Am. Chem. Soc.*, 2007, **129**, 10644–10645.
17 G. F. Manbeck and K. J. Brewer, *Coord. Chem. Rev.*, 2013, **257**, 1660–1675.
18 T. A. White, S. L. H. Higgins, S. M. Arachchige and K. J. Brewer, *Angew. Chem.*, 2011, **123**, 12417–12421.
19 T. A. White, B. N. Whitaker and K. J. Brewer, *J. Am. Chem. Soc.*, 2011, **133**, 15332–15334.
20 R. Zhou, G. F. Manbeck, D. G. Wimer and K. J. Brewer, *Chem. Commun.*, 2015, **51**, 12966–12969.
21 T. Stoll, M. Gennari, J. Fortage, C. E. Castillo, M. Rebarz, M. Sliwa, O. Poizat, F. Odobel, A. Deronzier and M.-N. Collomb, *Angew. Chem., Int. Ed.*, 2014, **53**, 1654–1658.
22 M. Karnahl, C. Kuhnt, F. W. Heinemann, M. Schmitt, S. Rau, J. Popp and B. Dietzek, *Chem. Phys.*, 2012, **393**, 65–73.
23 M. Karnahl, C. Kuhnt, F. Ma, A. Yartsev, M. Schmitt, B. Dietzek, S. Rau and J. Popp, *ChemPhysChem*, 2011, **12**, 2101–2109.
24 S. Rau, B. Schäfer, D. Gleich, E. Anders, M. Rudolph, M. Friedrich, H. Görls, W. Henry and J. G. Vos, *Angew. Chem., Int. Ed.*, 2006, **45**, 6215–6218.
25 H. Ozawa, M.-A. Haga and K. Sakai, *J. Am. Chem. Soc.*, 2006, **128**, 4926–4927.
26 H. Ozawa and K. Sakai, *Chem. Lett.*, 2007, **36**, 920–921.
27 H. Ozawa, Y. Yokoyama, M.-A. Haga and K. Sakai, *Dalton Trans.*, 2007, 1197–1206.
28 K. Sakai and H. Ozawa, *Coord. Chem. Rev.*, 2007, **251**, 2753–2766.
29 K. Sakai, H. Ozawa, H. Yamada, T. Tsubomura, M. Hara, A. Higuchi and M.-A. Haga, *Dalton Trans.*, 2006, 3300–3305.
30 M. G. Pfeffer, T. Kowacs, M. Wächtler, J. Guthmuller, B. Dietzek, J. G. Vos and S. Rau, *Angew. Chem., Int. Ed.*, 2015, **54**, 6627–6631.
31 M. G. Pfeffer, B. Schäfer, G. Smolentsev, J. Uhlig, E. Nazarenko, J. Guthmuller, C. Kuhnt, M. Wächtler, B. Dietzek, V. Sundström and S. Rau, *Angew. Chem., Int. Ed.*, 2015, **54**, 5044–5048.
32 P. Lei, M. Hedlund, R. Lomoth, H. Rensmo, O. Johansson and L. Hammarström, *J. Am. Chem. Soc.*, 2007, **130**, 26–27.
33 J. D. Knoll, S. M. Arachchige and K. J. Brewer, *ChemSusChem*, 2011, **4**, 252–261.
34 J. D. Knoll, S. L. H. Higgins, T. A. White and K. J. Brewer, *Inorg. Chem.*, 2013, **52**, 9749–9760.
35 M. T. Mongelli and K. J. Brewer, *Inorg. Chem. Commun.*, 2006, **9**, 877–881.
36 M. Toyama, K.-I. Inoue, S. Iwamatsu and N. Nagao, *Bull. Chem. Soc. Jpn.*, 2006, **79**, 1525–1534.
37 J. D. Knoll, S. M. Arachchige, G. Wang, K. Rangan, R. Miao, S. L. H. Higgins, B. Okyere, M. Zhao, P. Croasdale, K. Magruder, B. Sinclair, C. Wall and K. J. Brewer, *Inorg. Chem.*, 2011, **50**, 8850–8860.

